JOURNAL OF MATERIALS SCIENCE: MATERIALS IN MEDICINE **16** (2005) 719–726

Osteoblast cell adhesion on a laser modified zirconia based bioceramic

L. HAO[1,*], J. LAWRENCE[2], K. S. CHIAN[2]
[1]*Wolfson School of Mechanical and Manufacturing Engineering, Rapid Manufacturing Research Group, Loughborough University, LE11 3TU, UK*
E-mail: haoliang@pmail.ntu.edu.sg
[2]*Manufacturing Engineering Division, School of Mechanical & Production Engineering, Nanyang Technological University (NTU), 50 Nanyang Avenue, Singapore 639798*

Due to their attractive mechanical properties, bioinert zirconia bioceramics are frequently used in the high load-bearing sites such as orthopaedic and dental implants, but they are chemically inert and do not naturally form a direct bond with bone and thus do not provide osseointegration. A CO_2 laser was used to modify the surface properties with the aim to achieve osseointegration between bioinert zirconia and bone. The surface characterisation revealed that the surface roughness decreased and solidified microstructure occurred after laser treatment. Higher wettability characteristics generated by the CO_2 laser treatment was primarily due to the enhancement of the surface energy, particularly the polar component, determined by microstructural changes. An *in vitro* test using human fetal osteoblast cells (hFOB) revealed that osteoblast cells adhere better on the laser treated sample than the untreated sample. The change in the wettability characteristics could be the main mechanism governing the osteoblast cell adhesion on the YPSZ.
© *2005 Springer Science + Business Media, Inc.*

1. Introduction

Yttria partially stabilised zirconia (YPSZ) was introduced in the biomaterials world several years ago [1]. Zirconia bioceramics are frequently used in the high load-bearing sites such as artificial knee and bone screws in orthopaedic application and dental post crown in dental application due to their attractive mechanical properties [2]. Fini *et al.* [3] tested various materials in healthy and osteopenic bone, and YPSZ performed better when implanted in the healthy bone of rats. However, zirconia is chemically inert and does not bond with bone [4].

Events leading to integration of an implant into bone, and hence determining the performance of the implant, take place largely at the tissue-implant interface. The development of bone-implant interfaces depends on the direct interactions of bone matrix and osteoblasts with the biomaterial. There is a substantial body of literature based on the premise that improved initial attachment of osteoblasts or osteoblast precursor cells to orthopaedic implant surfaces may lead to improved bone integration of the implant and longer-term stability [5]. Properties of the biomaterial surface (such as topography and chemistry) control the type and magnitude of cellular and molecular events at the tissue-implant interface.

Different approaches are being used in an effort to obtain the desired surface properties of implants. Due to the rapid and specific modification of organic and inorganic materials, laser surface processing has aroused growing interests and been proven to be a controllable and flexible technique for modifying the surface properties of biomaterials. Lately, several publications have investigated the modification of biocompatibility of biomaterials' surface following laser irradiation. A CO_2 pulsed laser was used to graft polymer [6] and rubber [7]. The results showed a marked reduction in platelet adhesion and aggregation for modified polymer surface and cell attachment. The attached cells shows greater degree of spreading and flattening on the unmodified rubber surface. L929 fibroblast cells attached and proliferated extensively on the CO_2 and KrF laser treated films [8] in comparison with the unmodified PET, with surface morphology and wettability being found to affect cell adhesion and spreading. Hao and Lawrence recently have found that the enhanced wettability characteristics [9] caused by the CO_2 laser treatment brought about the favourable albumin [10] and fibronectin [11] protein adsorption response of the human fibroblast cell and human osteoblast cell on the laser modified magnesia partially stabilised zirconia (MgO-PSZ) [12, 13].

This aim of this study was to investigate the use of laser modification of YPSZ for improved osteoblast cell adhesion. It characterises the changes in the surface topography and wettability of YPSZ after irradiation with a 3 kW CO_2 laser. The human fetal osteoblast (hFOB)

*Author to whom all correspondence should be addressed.

cell line, which was established by transfection of limb tissue obtained from a spontaneous miscarriage, was used in an *in vitro* test. These osteoblast cells have the ability to differentiate into mature osteoblasts expressing the normal osteoblast phenotype. The cells provide a homogenous, rapidly proliferating model system for study normal human osteoblast differentiation, osteoblast physiology and hormonal, growth factor, and other cytokine effects on osteoblast function and differentiation. *In vitro* osteoblast cell adhesion revealed that there were more osteoblast cells adhered on the CO_2 laser treated YPSZ than on the untreated sample. The effects of the surface properties on the osteoblast cell adhesion were discussed.

2. Experimental procedures

2.1. Material and laser processing

The material under investigation was a 5% yttria partially stabilised zirconia (YPSZ) sheet with dimension of $10 \times 50 \times 5$ mm^3 (Dynamic Ceramic, Ltd.). It was used as received prior to laser treatment. A 3 kW CO_2 laser emitting a wavelength of 10.6 μm was used in this study. The laser was operated in the continuous wave (CW) mode and positioned by means of 2 linear axes (y- and z-axis) and 2 rotary axes (b- and c-axis). The defocused CO_2 laser beam was traversed in single time across the surface of the YPSZ samples placed on the state using the x-axis. A series of experiments was conducted for a wide range of power densities with an 11 mm spot diameter, whilst the traverse speed was set at 5000 mm/min with 2 bars pressure O_2 process gas.

2.2. Wettability analysis procedure

To investigate the effects of laser irradiation on the wetting and surface energy characteristics of the YPSZ, a set of sessile drop control experiments were carried out using glycerol, formamide, etheneglycol, polyglycol E-200 and polyglycol 15-200 with known total surface energy (γ_{lv}), dispersive (γ_{lv}^d) and polar (γ_{lv}^p) component values. The contact angles, θ, of the test liquids on the untreated and CO_2 laser treated YPSZ were determined in atmospheric condition at 25 °C using a sessile drop measure machine (First Ten Ångstroms, Inc). In order to estimate the influence of contaminant layers on the measurement results, the specimens of the untreated YPSZ were cleaned with acetone in an ultrasonic bath for 2 h, rinsed with distilled water several times and dried in a vacuum oven at 90 °C for 12 h. The test liquids were used to measure θ for the cleaned sample. It was observed that the value of θ on the cleaned sample are 1.5 °, 1.2 °, 1.0 °, 0.9 ° and 0.8 ° for glycerol, formamide, etheneglycol, polyglycol E-200 and polyglycol 15-200 respectively lower than that of the received sample without the cleaning. It is deemed that the contaminant on the surface of the YPSZ has only a slight influence on the value of θ. Since the contaminant is a minor factor active in the wettability characterisation, it is reasonable to preclude of cleaning pre-treatment for practical application of CO_2 laser treatment. In order to explore the potential of CO_2 laser treatment as an industrial and economical processing for altering the wettability of YPSZ, the current research is conducted in atmospheric environment without pre-cleaning. Each measurement of θ lasted for three minutes with profile photographs of the sessile drop obtained every minute and a mean value being subsequently determined. After the test liquid drops for each liquid attached and rested on the YPSZ surface, the drops consistently reached an equilibrium state in around 6 s. Thereafter they remained motionless and the magnitude of the θ changed little with time.

2.3. Osteoblast cell culture and adhesion

The human osteoblastic cell line hFOB 1.19 was obtained from the American Type Culture Collection (Manassas, USA). These cells were cultured in a medium containing a 1:1 mixture Dulbecco's Modified Eagle's medium without phenol red and Ham's F12 medium with 2.5 mM L-glutamine (D-MEM/F-12 Medium), supplemented with 10% fetal bovine serum (ATCC) and 0.3 mg/ml G418 (Calbiochem) in a 37 °C, humidified, 5% CO_2/95% air incubator. Osteoblasts at passage numbers 2–4 were used in this experiment. For osteoblast cell adhesion analysis, osteoblasts were enzymatically lifted from polystyrene tissue culture flasks until cell confluence using 1 ml Trypsin-EDTA (0.25% Trypsin/0.53 mM EDTA Solution) before suspension in the culture medium. The YPSZ samples were placed in a 24-well tissue culture polystyrene plate (Falcon, BP) under a sterile environment and sterilised in 70% ethanol for 24 h. The samples were rinsed by phosphate buffered salines (PBS) and then were seeded with cell suspension. The specimens were seeded with 0.5 ml cell suspension of 4×10^5 cell/mL and then cultured with cell culture medium and maintained in the incubator for one week. The cell culture medium was changed every 3 days. After incubation and gently rinsing with PBS, the samples with cells were fixed in 2.5% glutaraldehyde solution for one hour, washed with PBS, then dehydrated in increasing concentrations of alcohol and 100% acetone. The samples were dried in the Critical Point Dryer (CPD030, BAL-TEC) and then examined in the SEM (JEOL 5600LV) after sputter gold coating. Three untreated and CO_2 laser treated samples were prepared for each test. One typical SEM image for each untreated and CO_2 laser treated sample was chosen for analysis.

3. Results

3.1. Surface roughness and microstructure

The CO_2 laser treatment brought about a consistently smoother surface on the YPSZ sample compared with the untreated sample, as shown in Fig. 1(a). Surface roughness, R_a, decreased as the power density of laser treatment increased. The untreated YPSZ only showed grooves as evidence in Fig. 2(a) that may be generated in the manufacturing processing, while the microstructures appeared on the CO_2 laser treated samples as shown in Fig. 2(b) and (c). A hexagonal microstructure appeared on the sample treated at the 1.80 kW/cm^2, while a cellular microstructure appeared on the sample treated at the 2.25 kW/cm^2.

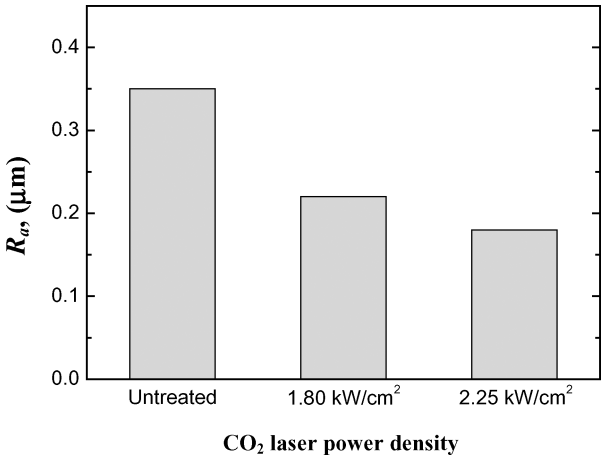

Figure 1 Relationship between the surface roughness and the CO_2 laser power density.

3.2. Wettability and surface energy

As shown in Table I, with all the control liquids used the YPSZ experienced an obvious reduction in contact angle as a result of interaction with the CO_2 laser treatment. The higher the power density applied, the lower θ obtained.

The intermolecular attraction which is responsible for surface energy, γ, results from a variety of intermolecular forces whose contribution to the total surface energy is additive [14]. The majority of these forces are functions of the particular chemical nature of a certain material, and as such the total surface energy comprises γ^p (polar or non-dispersive interaction) and γ^d (dispersive component; since van der Waals forces are present in all systems regardless of their chemical nature). Consequently the surface energy of any system can be described by [15]

$$\gamma = \gamma^d + \gamma^p \tag{1}$$

Therefore, the contact angle, θ, for solid-liquid systems where both dispersion forces and polar forces are present can be related to the surface energies of the respective liquid and solid by [15]

$$\cos\theta = \frac{2\left(\gamma_{sv}^d \gamma_{lv}^d\right)^{1/2} + 2\left(\gamma_{sv}^p \gamma_{lv}^p\right)^{1/2}}{\gamma_{lv}} - 1 \tag{2}$$

where γ_{lv}^p and γ_{lv}^d are the dispersive component and polar component of liquid surface energy, γ_{lv}, respectively, and, γ_{sv}^p and γ_{sv}^d are the dispersive component and polar component of solid surface energy, γ_{sv}, respectively. It is possible to adequately estimate γ_{sv}^d, for the YPSZ, by plotting the graph of $\cos\theta$ against $(\gamma_{lv}^d)^{1/2}/\gamma_{lv}$ according to Equation 2 as shown in Fig. 3. Thus, according to Fowkes [15], the value of γ_{sv}^d is estimated by the gradient $(= 2(\gamma_{sv}^d)^{1/2})$ of the line which connects the origin $(\cos\theta = -1)$ with the intercept point of the straight line ($\cos\theta$ against $(\gamma_{lv}^d)^{1/2}/\gamma_{lv}$) correlating the data point with the abscissa at $\cos\theta = 1$. Comparing the

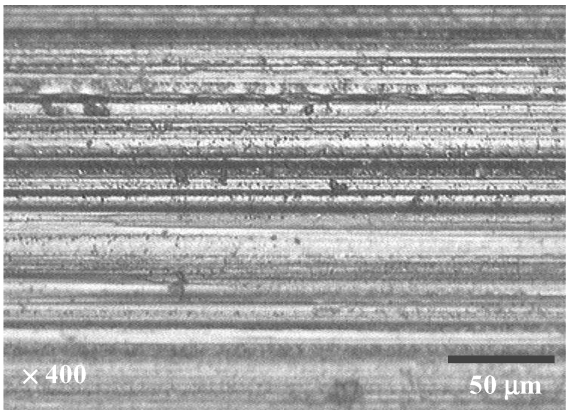

(a)

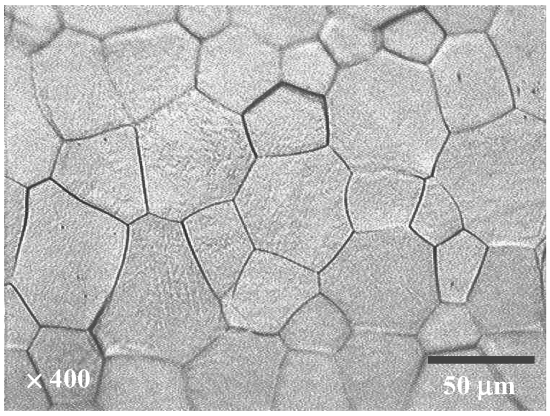

(b)

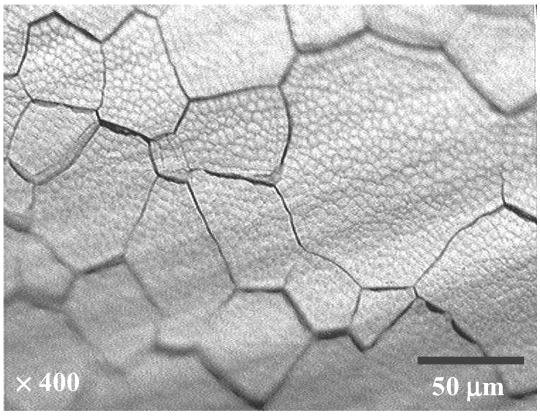

(c)

Figure 2 Optical image of the morphology of the (a) untreated YPSZ and CO_2 laser treated YPSZ with power densities of (b) 1.80 kW/cm^2, (c) 2.25 kW/cm^2

TABLE I Mean values of contact angles formed between the untreated and CO_2 laser treated YPSZ for various power densities and selected test liquids at 25 °C

	Glycerol	Formamide	Etheneglycol	Polyglycol E-200	Polyglycol 15–200
Untreated	82.4	76.2	64.4	56.8	40.2
CO_2 laser treated (1.80 kW/cm^2)	74.2	70.9	59.2	53.2	38.0
CO_2 laser treated (2.25 kW/cm^2)	70.5	67.7	57.0	49.8	36.9

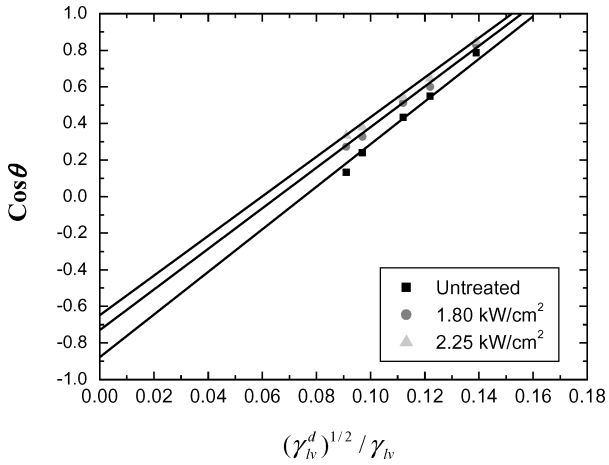

Figure 3 Plot of cos θ against $(\gamma_{lv}^d)^{1/2}/\gamma_{lv}$ for the untreated and CO_2 laser treated YPSZ in contact with the wetting test control liquids.

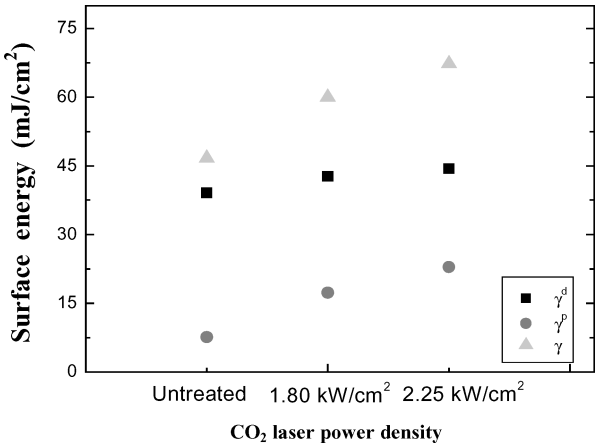

Figure 4 Relationship between surface energy (γ_{sv}^d, γ_{sv}^p and γ_{sv}) of the CO_2 laser treated YPSZ and power density.

ordinate intercept points of the untreated and CO_2 laser treated YPSZ-liquid systems in Fig. 3, it can been seen clearly that for the untreated YPSZ, the best-fit straight line intercepts the ordinate closer to the origin. This is noteworthy since intercept of the ordinate close to the origin is characteristic of the dominance of dispersion forces acting on the YPSZ material-liquid interfaces of the untreated and low power density treated sample, resulting in poor adhesion [15, 16]. On the other hand, the best-fit straight line of samples treated by the laser intercept the ordinate considerably high above the origin. An interception of the ordinate above the origin is indicative of the action of polar forces across the interface, in addition to dispersion forces, hence improved wettability and adhesion is promoted [15, 16]. Furthermore, because none of the best-fit straight lines intercept below the origin, it can be said that the development of an equilibrium film pressure of adsorbed vapour on the YPSZ surface (untreated and CO_2 laser-treated) did not occur [16].

It is not possible to determine the value of γ_{sv}^p for the YPSZ directly. Nonetheless, the following can be derived:

$$\left(\gamma_{sv}^p\right)^{1/2} = \frac{\left(\gamma_{sv}^d\right)^{1/2}(a-1)}{c} \tag{3}$$

a can be determined from the best-fit line of W_{ad} (Work adhesion) against W_{ad}^d (dispersive component of work adhesion) of the YPSZ, while c can be deduced from the best-fit line of γ_{lv}^p and γ_{lv}^d of the test liquids. For the YPSZ the value of a is 2.28 (untreated), 2.85 (1.80 kW/cm^2) and 3.10 (2.25 kW/cm^2), as c is 2.9 for the set of the test liquids defined previously [12]. It is therefore possible to calculate γ_{sv}^p for the YPSZ using Equation 3.

The determined results of surface energies of the untreated and CO_2 laser treated YPSZ (at various power densities) are given in the Fig. 4. As is evident from Fig. 4, CO_2 laser treatment increased γ_{sv} of the YPSZ by primarily increasing γ_{sv}^p, since γ_{sv}^d was similar for all the samples. It is important to note that because of the long range ionic interactions between the YPSZ and the test liquids, it is highly likely that the thermodynamically defined total solid surface energy, will be higher than the sum of the γ_{sv}^d and γ_{sv}^p components of the surface energy. Indeed, the derivation that leads to Equation 1 can only be done under the specific assumption that the ionisation potentials are all equal and that dipole-dipole random orientation interactions dominate over dipole-induced dipole random interactions. Although the increase in (excess) surface free energy will probably be less than the increase in the total lattice energy, on the other hand an absorbed liquid layer may shield the ionic fields substantially. As such, all the data derived from Equations 2 and 3 should be considered as being semi-empirical. Notwithstanding this, as the studies by many researchers [9, 17–19] found, it is reasonable to conclude from the data obtained from Equations 2 and 3 that CO_2 laser treatment of the YPSZ surface has caused an increase γ_{sv}^p.

3.3. Osteoblast cell adhesions

The hFOB human osteoblast cell adhesions improved considerably on the YPSZ after CO_2 laser treatment. As presented in Fig. 5, few osteoblast cells were found on the untreated YPSZ and covered less than 10% surface area of the sample. On the other hand, highly dense osteoblast cells appeared and covered about 70 and 90% surface area of the CO_2 laser treated YPSZ at

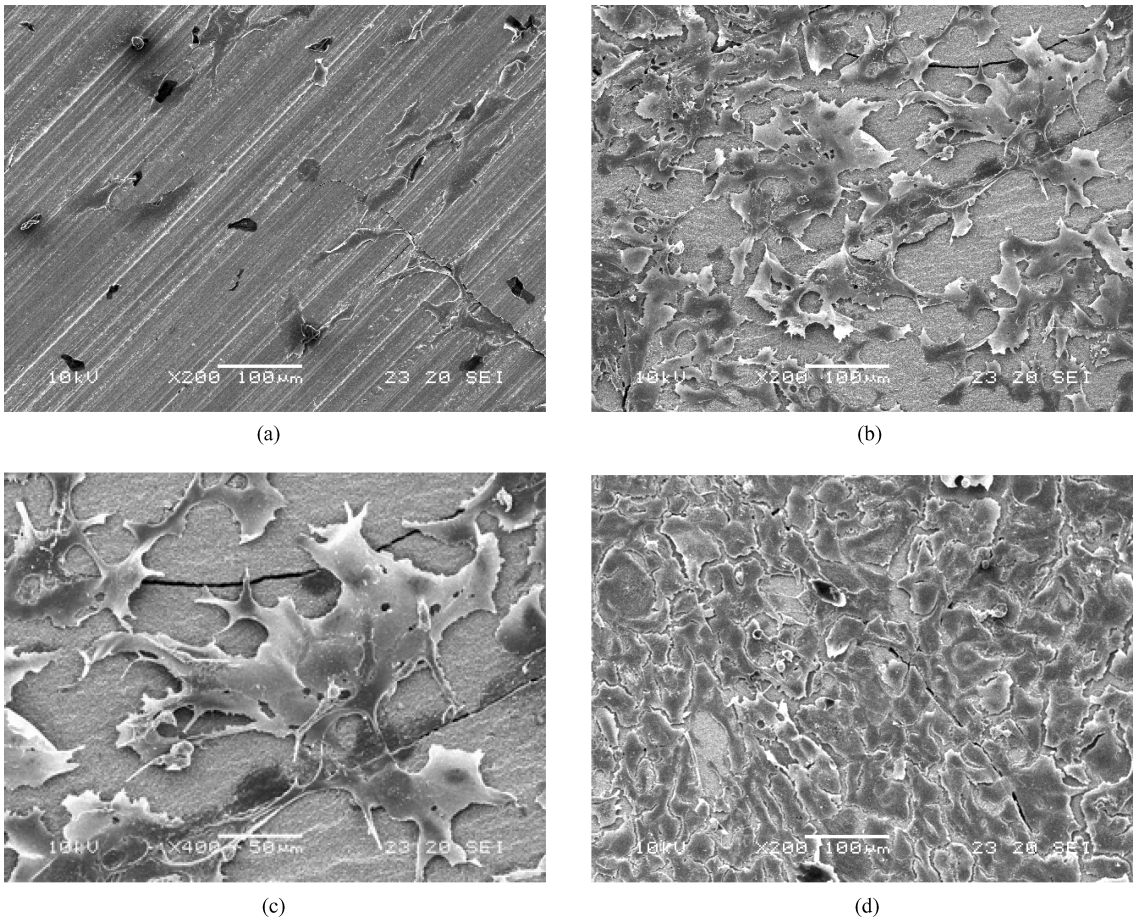

Figure 5 SEM image of hFOB human osteoblast cells on the (a) untreated YPSZ and CO_2 laser treated YPSZ at power densities of (b) 1.80 kW/cm^2, (c) 1.80 kW/cm^2 at high magnification and (d) 2.25 kW/cm^2.

1.80 kW/cm^2 and 2.25 kW/cm^2 respectively. In addition, the morphology of osteoblast cells on the CO_2 laser treatment showed better spreading on the CO_2 laser treated sample compared with the cells on the untreated sample. The typical osteoblast cells on the CO_2 laser treated sample at 1.80 kW/cm^2, as observed in Fig. 5(c), had spread completely and flatten, with the cytoplasmic spread to cover larger area and elongated filopodias. On the other hand, the osteoblast cells on the untreated sample did not show good spreading and filopodias as shown in Fig. 5(a).

It is very interesting to note that two osteoblast cells adhered in one of the grooves generated by the polishing methods employed by the manufacturers of the YPSZ. The groove in question had a width of about 10 μm and the two osteoblast cells spread along the direction of the groove and connected with each other as shown in Fig. 6. Such an observation implies that the surface topography could influence the direction of osteoblast cell spreading and growth.

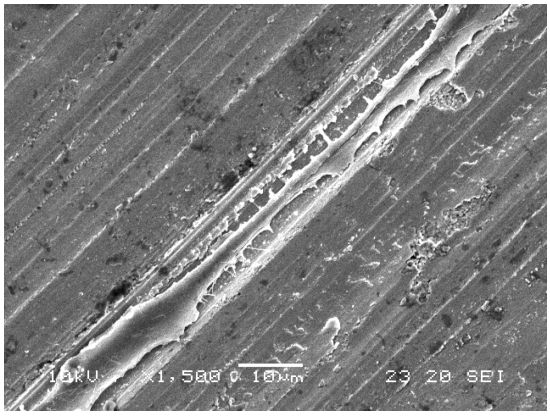

Figure 6 SEM image of two hFOB human osteoblast cells' spreading and connection in the groove.

4. Discussions

Because intense local heating brought about by the interaction with incident CO_2 laser beam could result in the melting and thus erase the grooves of the YPSZ, a smoother surface was generated by the CO_2 laser treatment. The higher power density of the CO_2 laser treatment brought about the high extent melting and smoother surface of the YPSZ. Furthermore, the surface of the modified YPSZ showed a typical microstructure of rapid solidification after CO_2 laser irradiation. A high heat input from a laser beam facilitates surface localized melting at a very high efficiency. That is, the major portion of the absorbed energy is used for melting, with only a small fraction going into the heating of the solid sub-surface material. This ability to maintain a cold substrate whilst melting a thin surface layer of material results in rapid quenching of the molten layer once the beam is removed. Thermal gradients, G, at liquid-solid interface layer are very steep. In this case,

melt solidification is almost a self-quenching process as a constitutional supercooling. With the increasing CO_2 laser power density, the degree of the constitutional supercooling increased which caused the developing stages of cellular structure. At the power density of 1.80 kw/cm^2, the capped-hexagonal formation becomes the interface. When marked supercooling exists at power density of 2.25 kw/cm^2, the cellular structure developed as shown in Fig. 2. Indeed, different solidified microstructures generated by laser irradiation have been reported by a number of workers conducting research into the laser treatment of various ceramics. Pei *et al.* [20] noted that both equiaxed and dendritic microstructures were obtained in different regions of the same laser clad ZrO_2 layer, concluding that the differences were related to different cooling rates in the various regions of the laser clad ZrO_2 layer. Liu [21] obtained similar results in laser sealing Y_2O_3-ZrO_2 and MgO-ZrO_2 ceramic coatings. Hao and Jonathan found the difference microstructure on the MgO-PSZ generated at the different CO_2 power densities [22]. Such differences in microstructure type and size were ascribed to the varying degrees of constitutional supercooling, which, according to McCallum *et al.* [23], are inherent in laser processes.

A model similar to that for heterogeneous solid surfaces can be developed in order to account for surface irregularities, being given by Wenzel's equation [24]:

$$r_a(\gamma_{sv} - \gamma_{sl}) = \gamma_{lv} \cos\theta_w \tag{4}$$

where r_a is the roughness factor defined as the ratio of the real and apparent surface areas and θ_w is the contact angle for the wetting of a rough surface. It is important to note that Wenzel's treatment is only effective at the position of the wetting triple line [24]. Equation 4 shows that if r_a is big, that is the solid surface is rough, then $\cos\theta_w$ is large and θ_w decrease when $\theta_w < 90^\circ$. However, in this study, the smooth surface generated by the CO_2 laser treatment had the lower θ than the rough untreated surface. It contradicts with Equation 4 and previous work [25] that an increase in surface roughness effected a decrease in θ and enhanced the wettability. It must be noted that the experimental conditions in the place in this study and in the previous work by others are very different. Whereas in the previous work only the surface roughness was altered, in this work the CO_2 laser treatments brought about changes in surface energy and surface roughness simultaneously. Hence, it implies that the surface energy might play a predominant role in wettability characteristics of YPSZ.

A clear relationship between the value of $\cos\theta$ and the surface energy can be observed in Fig. 7, which reveals that an increase in the surface energy will cause a rise in $\cos\theta$. Therefore, it is deemed that the surface energy primarily influences the wettability of the YPSZ. Indeed, it was found by Lawrence [26] that surface energy was the most predominant factor governing the wetting characteristics of the SiO_2/Al_2O_3-based ceramic following the irradiation of high power diode laser. What's more, Hao and Lawrence recently found that the change in surface energy, represented the change in microstructure feature [27], was identified as the main mechanism governing the wettability characteristics of the MgO-PSZ following CO_2 laser irradiation [28]. Since γ_{sv}^d only changed slightly after laser treatment as shown in Fig. 4, a significant increase in the total surface energy were governed by the mark enhance in the γ_{sv}^p. The increase in γ_{sv}, in particular the increase in γ_{sv}^p, have a positive effect upon the action of wetting and adhesion [29], since primarily both dispersion and polar forces are active to a greater extent [15, 16]. The changes in γ_{sv} are thought to be due to the fact that CO_2 laser treatment of the YPSZ results in the surface melting of the surface; a transition that is known to effect an increase in γ_{sv}^p [30], and thus an improvement in the wettability and an increase in the adhesion at the interface in contact with the control liquids. Especially, the solidified microstructure generated by laser surface melting might be attributed to the changes in surface energy and thereof in wettability characteristics. The surface energy of samples with hexagonal structure and cellular structure is 60 and 67.3 mJ/cm^2 respectively and higher than the untreated sample with the surface energy of 46.7 mJ/cm^2. Indeed, work conducted by Zhang *et al.* [31] found that considerable improvement in the bond strength of a Si_3N_4 ceramic could be realised only when excimer laser treatment of a structural alloy steel (SAE 4340) resulted in surface melting. Similarly, Lawrence [26] observed a sharp reduction in θ at the point of melting for an Al_2O_3/SiO_2 based oxide compound after high diode power laser (HPDL) treatment.

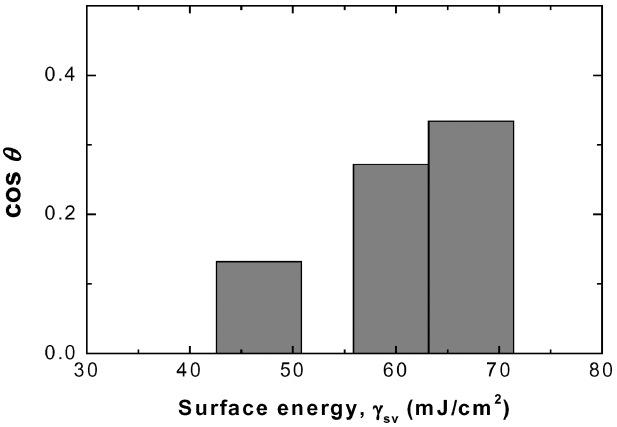

Figure 7 The relationship between wettability characteristics ($\cos\theta$, glycerol) and surface energy of the YPSZ.

Cell coverage density, represented by the ratio of osteoblast cell covered area and the whole surface area, is used to express the degree of osteoblast cell adhesion. There are higher cell cover densities on the samples following CO_2 laser treatment than on the untreated sample as shown in Fig. 8. In the power density range employed and in the specified experimental conditions, the increase in power density caused an increase in cell cover density. It is certain that the levels of power densities of the CO_2 laser treatment are a significant factor in promoting the hFOB human osteoblast cell adhesion, implying that this technique is able to improve the response of the cells to the YPSZ. Indeed, the CO_2 laser treatment creates the changes in the topography and surface energy synchronously. These changes,

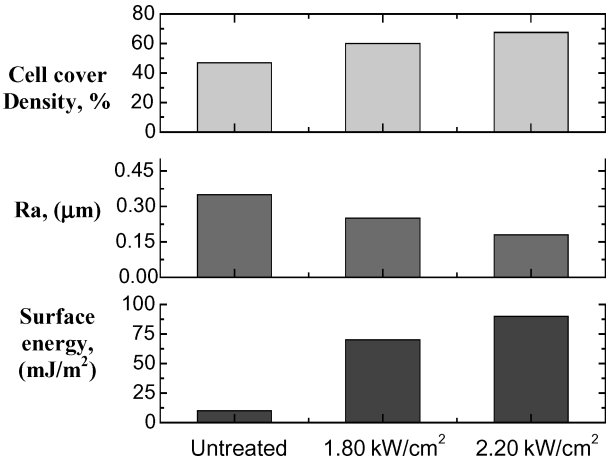

Figure 8 The relationship between the osteoblast cell cover density, surface roughness (R_a), surface energy and CO_2 laser power densities.

which primarily determined the wettability characteristics, could be the factors influencing the response of the hFOB human osteoblast cells.

The CO_2 laser treatment generated a consistently smoother surface on the YPSZ compared to the untreated sample. R_a increased with the power density of CO_2 laser treatment. As shown in Fig. 8, the CO_2 laser treated YPSZ with smoother surface had higher cell cover density compared to the smooth untreated sample. This contradicts some reports demonstrating that the rougher surface promoted more osteoblast-like cell attachment on titanium [32], apatite-wollastonite glass ceramic [33] and hydroxyapatite [34]. Hence, one could assume that surface roughness is not the primary factor influencing human osteoblast cell adhesion on the laser treatment YPSZ, since the smoother surface clearly had better cell response than rougher ones, because other surface properties beside surface roughness also changed after laser treatment in this study. It is postulated that others factors may exert more influence on cell response than the surface roughness based on the facts that the relationship between the cell coverage density and surface roughness nd was not in accordance with previous results of Ohgushi *et al.* [33] and Deligianni *et al.* [34].

Although the macrotopography presented by surface roughness does not influence cell adhesion significantly, it is found that the microtopography could affect the cell spreading as shown in Fig. 6. The spreading of the cells could be defined in the groove and along the direction of the groove with about 10 μm. A previous finding revealed that the surface topography also caused the alignment of cells parallel to the 10 μm grooves present on the metal surfaces [35]. Surface microtopography has been cited as an important factor influencing protein-surface and cell-surface interactions [36]. Curved surfaces, pits, protrusions, cavities, etc., that have sizes and radii comparable with those of the biological entities (proteins $\sim$1–10 nm, cells 1–100 μm) induce biological interactions different from those on a flat surface [36]. It is noted that the degrees of the cell adhesion improved markedly when obvious microstructural change occurred on the YPSZ. The 70 and 90% cell cover densities occurred on the laser modified surface with hexagonal and cellular microstructure respectively. A number of reasons have been suggested for an increased differentiation of osteoblasts on microstructured surface, such as the influence of surface structure on cell shape or that the surface topography creates a specific bio-chemical microenvironment around each cell [37]. Microstructures about 10–20 μm induced by the CO_2 laser treatment on the polyethylene terephthalate (PET) were regarded as one of the factors influencing the fibroblast cell attachment and spreading [38].

As one can see from Fig. 8, the cell adhesion increases as the surface energy of YPSZ increase. There were only sparsely adhered cells on the untreated sample with surface energy of 46.7 mJ/cm^2, an obvious improvement of cell adhesion were found on the CO_2 laser treated YPSZ with surface energy of 60 mJ/cm^2 and while maximal cell adhesion occurred on the YPSZ with surface energy of 67.3 mJ/cm^2. The work on polymers and glass revealed that cell spreading and substratum surface free energy showed a characteristic sigmoid relationship both in the presence and in the absence of serum proteins; good spreading only occurred when surface energy higher than approximately 57 mJ/cm^2 [39]. It was found that the critical parameter for osteoconduction was the initial number of well-attached osteoblastic cells to the bone substitute [40]. Therefore, the difference in cell adhesion was attributed to the difference in wettability characteristics, which is determined by the surface energy, particularly the polar component between the untreated and CO_2 laser treated YPSZ. Since the change in wettability characteristics was primarily influenced by the surface energy of the YPSZ, especially polar component. The finding agrees with previous studies showing the influence of wettability on various cells attachment and spreading [32, 40–42].These studies showed good cell attachment and spreading on high-energy substrata and poor cell attachment and spreading on low-energy substrata, which accounts for the minimal energetic state of a system in equilibrium. The finding in the behaviour of osteoblastic cells at the surface of HA [40] and at the surface of titanium [32] demonstrated that γ^p play a critical role. As shown in Fig. 4, the dispersion components (γ^d) in surface energy were similar, whereas the polar components were significantly different for the untreated and CO_2 laser treated YPSZ at various power densities. Therefore, the change in the osteoblast cell adhesion was mainly related to γ^p. These results indicated that γ^p influenced the behaviour of osteoblasts on YPSZ surfaces more strongly compared to γ^d, which was probably attributed to the fact that the composition of the culture medium all are polar, and thus osteoblast cells and YPSZ should interact mainly in polar force. Moreover, the osteoblast cells showed better spreading and flattened at the CO_2 laser treated sample. It is likely that the more flattened osteoblast cells produced more collagen than less flatted osteoblast cells [40] on the untreated sample. One important aspect to be considered in this study is the kinetics of osteoblast cell events. The difference in morphology of osteoblast cell attachment might lead to the difference in terms of

osteoblast cell growth. It was suggested that enhancing polar component of surface energy would promote the initial osteoblast cell attachment and spreading, and thereby could bring about a large bone-like matrix synthesis.

5. Conclusions

With the aim being to achieve osseointegration at the bioinert zirconia and bone interface, a CO_2 laser was used to modify the surface properties of an yttria partially stabilised zirconia (YPSZ) bioceramic. It was found that the surface roughness decreased and solidified microstructure occurred after laser treatment. Furthermore, the CO_2 laser treatment generated higher wettability characteristics, represented by the lower contact angle with test liquids, which was primarily due to the enhancement of the surface energy, particularly the polar component, determined through microstructural changes. An *in vitro* test using hFOB human osteoblast cells revealed better cell adhesion on the laser treated sample than on the untreated sample. Although surface roughness plays a minor role in the osteoblast cell adhesion, the microtopography could influence the osteoblast cell spreading in terms of the grooves and cell adhesion in terms of microstructure. Moreover, the change in the wettability characteristics could be the main mechanism governing the osteoblast cell adhesion on the YPSZ.

References

1. P. S. CHRISTEL, *Bull. Hosp. Joint Diseas. Orthop. Inst.* **49** (1989) 170.
2. J. LI and G. W. HASTINGS, "Oxide Bioceramics: Inert Ceramic Materials in Medicine and Dentistry," Chapman & Hall: London, New York (1998) p. 340.
3. M. FINI, N. NICOLI ALDINI, M. G. GANDOLFI, M. MATTIOLI BELMONTE, G. GIAVARESI, C. ZUCCHINI, A. DE BENEDITTIS, S. AMATI, A. RAVAGLIOLI and E. T. KRAYEWSKI, *Inter. J. Artif. Org.* **20** (1997) 291.
4. T. J. WEBSTER, R. W. SIEGEL and R. BIZIOS, *Biomaterials* **20** (1999) 1221.
5. D. A. PULEO and R. BIZIOS, *J. Biomed. Mater. Res.* **26** (1992) 291.
6. H. MIRZADEH, A. A. KATBAB and R. P. BURFORD, *Rad. Phy. Chem.* **46** (1995) 859.
7. H. MIRZADEH, A. A. KATBAB, M. T. KHORASANI, R. P. BURFORD, E. GORGIN and A. GOLESTANI, *Biomaterials* **16** (1995) 641.
8. M. DADSETAN, H. MIRZADEH, N. SHARIFI-SANJANI and M. DALIRI, *J. Biomed. Mater. Res.* **57** (2001) 183.
9. L. HAO and J. LAWRENCE, *J. Phys. D.* **36** (2003) 1292.
10. L. HAO and J. LAWRENCE, *Colloids Surf. B: Biointerf.* **34** (2004) 87.
11. L. HAO and J. LAWRENCE, *J. Biomed. Mater. Res.* **69A** (2004) 748.
12. L. HAO and J. LAWRENCE, *Mate. Sci. Engng. C* **23** (2003) 627.
13. L. HAO, J. LAWRENCE and K. S. CHIAN, *J. Biomater. Appl.* **19** (2004) 81.
14. N. K. ADAM and G. E. P. ELLIOTT, *J. Chem. Soc.* **18** (1958) 2206.
15. F. M. FOWKES, *Ind. Eng. Chem.* **56** (1964) 40.
16. J. R. DANN, *J. Colloid Interf. Sci.* **32** (1970) 302.
17. S. AGATHOPOULOS and P. NIKOLOPOULOS, *J. Biomed. Mater. Res.* **29** (1995) 421.
18. J. LAWRENCE and L. LI, *J. Phys. D* **32** (1999) 1075.
19. J. LAWRENCE, L. LI and J. T. SPENCER, *Appl. Surf. Sci.* **138/139** (1999) 388.
20. Y. T. PEI, J. H. OUYANG and T. C. LEI, *Surf. Coat. Techn.* **81** (1996) 131.
21. Z. LIU, "Surface Modification of Materials Using High Power Lasers and An Arc Image Intensifier," PhD Thesis, University of Liverpool, 1991.
22. L. HAO and J. LAWRENCE, in Proceedings of the IMechE Part B, J. Eng. Manufacture. (2004) vol. 218.
23. R. W. MCCALLUM, M. J. KRAMER and S. T. WEIR, *IEEE Trans. Appl. Supercond.* **3** (1993) 1147.
24. R. N. WENZEL, *Ind. Eng. Chem.* **28** (1936) 988.
25. T. UELZEN and J. MULLER, *Thin Solid Films* **434** (2003) 311.
26. J. LAWRENCE, *Proc. Royal Soc. London, Series A* **458** (2002) 2445.
27. L. HAO and J. LAWRENCE, *Mater. Sci. Engng. A.* **364** (2003) 171.
28. *Idem., J. Laser Appl.* Submitted for publication (2003).
29. A. W. NEUMANN, *Adv. Colloid Interf. Sci.* **4** (1974) 106.
30. D. K. CHATTORAJ and K. S. BIRDI, "Adsorption and the Gibbs Surface Excess" (Plenum Press: New York, 1984) p. 95.
31. X. M. ZHANG, T. M. YUE and H. C. MAN, *Mater. Lett.* **30** (1997) 327.
32. B. FENG, J. WENG, B. C. YANG, S. X. QU and X. D. ZHANG, *Biomaterials* **24** (2003) 4663.
33. H. OHGUSHI, Y. DOHI, T. YOSHIKAWA, S. TAMAI, S. TABATA, K. OKUNAGA and T. SHIBUYA, *J. Biomed. Mater. Res.* **32** (1996) 341.
34. D. D. DELIGIANNI, N. D. KATSALA, P. G. KOUTSOUKOS and Y. F. MISSIRLIS. *Biomaterials* **22** (2001) 87.
35. M. AHMAD, D. GAWRONSKI, J. BLUM, J. GOLDBERG and G. GRONOWICZ, *J. Biomed. Mater. Res.* **46** (1999) 121.
36. B. KASEMO and J. GOLD, *Adv. Dent. Res.* **13** (1999) 8.
37. B. CHEHROUDI, J.-L. QU and D. M. BRUNETTE, "Effects of Implant Surface Topography on Osteogenesis," in: Proceedings of the 5th World Biomaterials Congress, May 29-Jun 2 1996 (Toronto, Canada, 1996).
38. H. MIRZADEH and M. DADSETAN, *Radiation Phys. Chem.* **67** (2003) 381.
39. J. M. SCHAKENRAAD, H. J. BUSSCHER, C. R. H. WILDEVUUR and J. ARNDS, *J. Biomed. Mater. Res.* **20** (1986) 773.
40. S. A. REDEY, M. NARDIN, D. BERNACHE-ASSOLANT, C. REY, P. DELANNOY, L. SEDEL and P. J. MARIE, *J. Biomed. Mater. Res.* **50** (2000) 353.
41. C. A. SCOTCHFORD, E. COOPER, G. J. LEGGETT and S. DOWNES, *ibid.* **41** (1998) 431.
42. R. L. PRICE, M. C. WAID, K. M. HABERSTROH and T. J. WEBSTER, *Biomaterials* **24** (2003) 1877.

Received 5 April
and accepted 18 November 2004